Journal of Applied Physics

Self-excited electrostatic pendulum showing electrohydrodynamic-force-induced oscillation

Cite as: J. Appl. Phys. **122**, 243302 (2017); https://doi.org/10.1063/1.5003010
Submitted: 01 September 2017 . Accepted: 09 December 2017 . Published Online: 27 December 2017

Karl D. Stephan, and José M. Hernandez Guerrero

AIP Publishing

Self-excited electrostatic pendulum showing electrohydrodynamic-force-induced oscillation

Karl D. Stephan[a] and José M. Hernandez Guerrero
Ingram School of Engineering, Texas State University, San Marcos, Texas 78666, USA

(Received 1 September 2017; accepted 9 December 2017; published online 27 December 2017)

The electrohydrodynamic (EHD) effect ("ion wind") associated with corona discharges in air has been extensively investigated and modeled. We present a simple experiment that shows how both the magnitude and direction of EHD forces can change in such a way as to impart energy continuously to an oscillating electrostatic pendulum. The amplitude of oscillations of an electrostatic pendulum subject to EHD forces can grow approximately exponentially over a period of minutes, and we describe a qualitative theory to account for this effect, along with implications of these experiments for theories of ball lightning. *Published by AIP Publishing.*
https://doi.org/10.1063/1.5003010

I. INTRODUCTION

The mechanical effects of a corona discharge have been known since at least 1750, when Wilson invented the electric pinwheel.[1] More recently, electrohydrodynamic (EHD) effects have been studied for both drag reduction on conventional aircraft[2] and as thrusters for propulsion.[3] Because the magnitude of forces involved in most atmospheric-pressure EHD experiments is small, sensitive and sophisticated instrumentation is often needed to measure these forces accurately and repeatably. Saranin[4] has shown that an easily constructed electrostatic pendulum is capable of demonstrating complex and subtle behavior, including nonlinear oscillations that conform to theoretical predictions. While Saranin's work did not involve the measurement of EHD forces, he showed that an electrostatic pendulum could be useful for delicate measurements.

We present data from experiments with a simple two-degrees-of-freedom electrostatic pendulum consisting of a ball bearing suspended by a thin conducting wire. With sufficient voltage applied, a corona appears on the wire and produces ions that give rise to EHD forces. The system's equilibrium becomes unstable and initial motion of the pendulum produces an asymmetry in the EHD forces, leading to oscillations that grow in amplitude approximately exponentially over a 4-min observation time.

II. METHODS

The setup used is shown in Fig. 1. All experiments were performed inside a 277 mm-ID × 313-mm-inside-height aluminum vacuum chamber to avoid external drafts. Ambient laboratory air at atmospheric pressure was maintained in the chamber at all times. A clear acrylic chamber lid permitted the connection of a high-voltage feedthrough from an external power supply to a 79-μm-diameter enamel-insulated copper wire (#40 AWG) wound on a windlass cylinder suspended between two foam-plastic supports.

(The extremely thin insulation on the wire does not withstand the electric fields produced in this experiment, so its presence is immaterial and allows DC current flow as though the wire was not insulated.) The pendulum wire ran from the windlass through a triangular slot in a plastic beam that formed a stationary fulcrum from which the pendulum length was measured. A 5.96-mm-diameter steel ball bearing was soldered to the wire and served as the pendulum weight. The mass of the ball bearing and solder was $m = 860$ mg.

Because the output polarity of the high-voltage supply (Information Unlimited HV-50P) with respect to ground was positive and we wished to apply both positive and negative polarities to the pendulum, we placed a small insulated platform underneath the pendulum, about 16 mm below the bottom of the weight. This platform consisted of an 80-mm-diameter copper-clad fiberglass sheet whose edges were covered with 6.3-mm-diameter copper tubing, slotted to fit over the edges. The resulting rounded edge of the platform prevented corona discharge from the platform that might cause interfering air currents. Because connections to both the pendulum and the platform were insulated to at least 20 kV with respect to the grounded chamber, a high voltage of either polarity could be applied to the pendulum with respect to the platform.

Video cameras were used to capture the motion of the pendulum. The clear acrylic chamber lid permitted an unobstructed view of the ball bearing hanging above the platform from above the chamber (Fig. 2). Also, a small hole on the side of the chamber near the bottom (not shown in Fig. 1) allowed photography from the side as well. Videos at frame rates varying from 3.83 s^{-1} up to 500 s^{-1} were taken of the pendulum oscillations. The horizontal and vertical directions of the top-view video image were taken as the arbitrary orthogonal x- and y-axes of pendulum motion. Because the camera was not directly above the pendulum, the pixel-to-cm scale ratio was slightly different in the x- and y-directions, and this difference was taken into account with calibration images of known-length scales placed on the platform. The location of the ball bearing in each video image was digitized manually by means of the open-source

[a]Email: kdstephan@txstate.edu

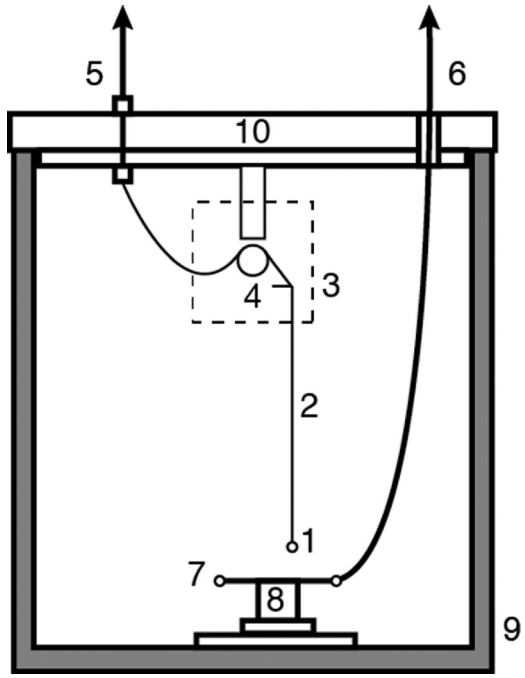

FIG. 1. Setup used for electrostatic pendulum experiments. *1*—pendulum weight (5.96-mm-diameter ball bearing), *2*—suspension wire (79-μm-diameter copper), *3*—foam plastic support for windlass and fulcrum, *4*—plastic windlass, *5*—HV terminal connecting to pendulum, *6*—HV insulated cable connecting to insulated platform, *7*—copper-clad insulated platform, *8*—plastic platform insulator, *9*—aluminum vacuum chamber wall (always connected to negative HV terminal), and *10*—acrylic chamber lid.

image processing software ImageJ (https://imagej.nih.gov/ij/) maintained by the U.S. National Institutes of Health. A small bright dot corresponding to the reduced-size reflection of a room light was used as the ball's position reference for the digitizing process, as any rotation of the spherical bearing would not affect the angular position of the reflection. At the scale used for most of the images, 1 pixel corresponded to about 10 μm of ball motion. For most of the experiments, the effective length of the pendulum (from the fulcrum to the pendulum's center of mass) was $l = 161.5$ mm. This corresponds to a natural frequency for the unforced pendulum of $f_0 = (1/2\pi)(g/l)^{1/2} = 1.2398$ Hz, using the small-angle linearized formula for a pendulum's period and assuming the acceleration of gravity $g = 9.8\ \mathrm{m\ s^{-2}}$.

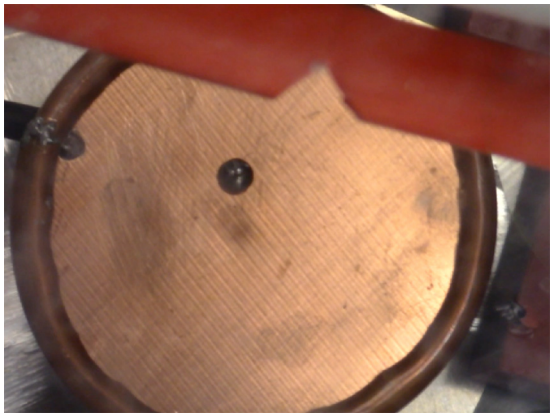

FIG. 2. Frame from video taken of the ball-bearing pendulum above the platform. Suspension wire passes through the triangular notch shown at the top of the photo.

The applied DC voltage and resulting corona current were monitored with the circuit shown in Fig. 3. A Tektronix P6015A high-voltage probe was connected to a Tektronix TDS-2024B oscilloscope to monitor the applied voltage magnitude, and a 100-kΩ current-sensing resistor in series with the return lead was used to monitor current by means of the resistor's voltage drop. While it is possible that not all the corona current emitted by the wire was collected by the platform when the wire was positive and both the platform and the chamber were negative, enough current was collected to provide a relative measurement of the wire's corona current even in that case. Because of the way the setup wiring was configured, it was not possible safely to obtain separate current measurements for the chamber current and the platform current.

During a typical experiment, the digital video camera recording was started 10 s before the high voltage (HV) power was applied, in order for a record to be made of the neutral-point position in the absence of an electric field or corona. It was not possible to remove absolutely all motion from the pendulum prior to an experiment, but a typical amplitude of oscillation before the application of power was <0.2 mm (peak-to-peak). Simultaneously with the application of high voltage, a fiber-optic indicator in the camera's field of view provided a power-on time reference, and the motion of the pendulum was recorded for subsequent times ranging from a few seconds to almost 4 min.

Initially, the location of the corona producing the motion was uncertain. We used a low-light monochrome video camera (Watec model 124N+) to make time exposures of the lower part of the pendulum through the small hole in the side of the chamber. Figure 4 shows a 10-s time exposure during which the pendulum was oscillating slightly. The corona discharges along the wire traced out elliptical rings above the

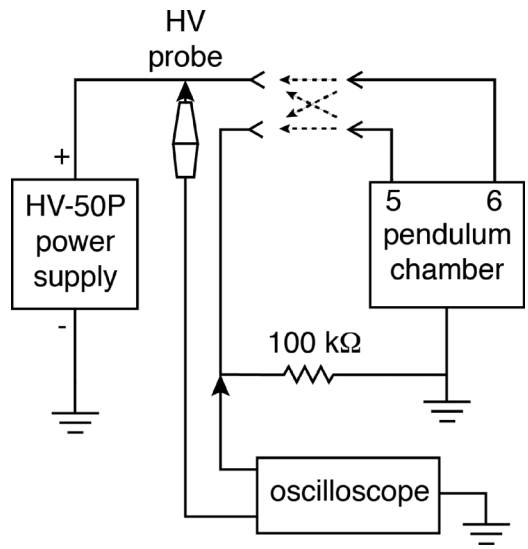

FIG. 3. Schematic diagram of electrical connections used to monitor the corona discharge of the electrostatic pendulum. The dashed arrows show alternative connections for applying both positive and negative voltages to the pendulum. Numbers 5 and 6 correspond to those shown in Fig. 1.

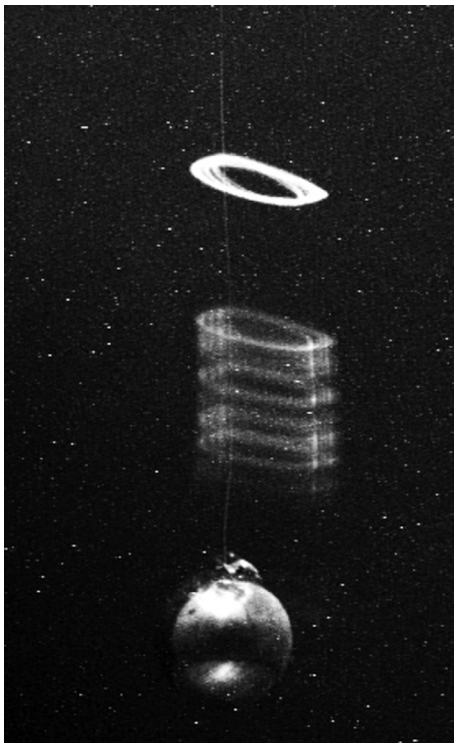

FIG. 4. 10-s time exposure of the oscillating pendulum, showing corona along the suspension wire above the ball (exposed with separate flash during time exposure). The pendulum was at +15 kV with respect to the platform and chamber. The white dots are camera artifacts (leaky pixels that appear in long time exposures).

ball bearing, which was exposed to a short-duration flashlamp flash to show its relative position with regard to the corona, which was too dim to see with the unaided eye.

To confirm that corona was indeed responsible for the growing oscillations we observed, we temporarily enclosed the suspension wire inside a 6.3-mm-diameter copper sleeve that covered the wire from the pendulum weight to within a few mm of the fulcrum. Tests up to 20 kV produced no DC corona current from the much thicker conductor, and the pendulum with the thicker conductor showed no evidence of growing oscillations.

III. RESULTS

To limit the total amount of data to be manually analyzed for each experiment, we restricted each experimental run to about 1000 video frames. A frame rate of 15.31 s^{-1} therefore allowed 1 min of video to be captured. We took a series of runs of this length, varying the voltage applied to the wire from −18 kV to +18 kV by 3-kV steps. The I-V curves for both positive and negative applied voltage fit well the theoretical behavior of a thin-wire corona discharge as described in, e.g., Fridman and Kennedy,[5] in which the corona current I and corona voltage V are related by the constants K (A V^{-2}) and the critical voltage V_{cr} for voltages $V > V_{cr}$, namely $I = KV(V - V_{cr})$. As the data in Fig. 5 show, the experimental data agree very well with the theoretical curves fit to them. In Fig. 5, the HV polarity refers to the polarity of the pendulum with respect to the platform, the chamber always being connected directly to the negative

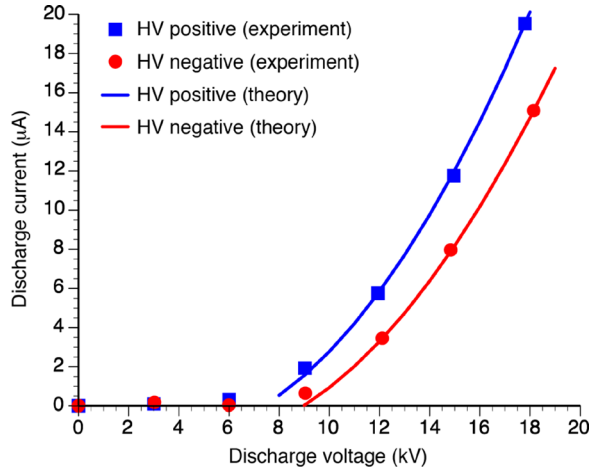

FIG. 5. Experimental *I-V* data for the electrostatic pendulum setup (squares = pendulum positive, circles = pendulum negative). The theoretical curves are derived as described in the text.

terminal of the power supply. The constants used for the fitted curves were $K_+ = 0.105\,\mu$A kV^{-2}, $K_- = 0.0905\,\mu$A kV^{-2}, $V_{cr+} = 7.349$ kV, and $V_{cr-} = 8.962$ kV. The differences between the curves for positive and negative corona can be attributed to two factors: (1) the fact that the critical breakdown voltage for DC corona is lower for positive than for negative corona due to the different nature of the respective breakdown mechanisms (see, e.g., Cobine[6]) and (2) because only the platform current and not the chamber current was monitored with the wire positive, some current with the wire positive may have passed directly to the chamber, bypassing the platform and its current-monitoring resistor. These factors do not alter the main conclusion we draw from Fig. 5, which is that corona is present on the suspension wire for sufficient voltages of both polarities applied to it.

If the system was operating in a vacuum and no DC current flow was possible, some initial pendulum motion would occur when high voltage is applied for the following reason. It proved impossible to make the setup exactly axially symmetrical so that when voltage is applied, all electrostatic forces due to the conducting objects surrounding the pendulum would exactly cancel. Therefore, even in a vacuum, when high voltage is applied the pendulum would move from its gravitational neutral point (point of lowest energy) to a slightly different location (the "power-on" neutral point) due to residual asymmetries in the electric-field environment. But after this initial motion, the pendulum's oscillations would be damped out by mechanical friction and would eventually die away. No further transfer of energy to the pendulum from a DC high-voltage supply would be possible in the absence of ionized air.

Such initial motion followed by damped oscillations is exactly what happens when voltage is applied in air as well, up to the point that the suspension wire begins to emit corona current, which occurs in this case at a voltage of about 7.3 kV (for positive corona) or 8.9 kV (for negative corona). The raw x-coordinate data (in cm) for the experiment in which +9 kV was applied at $t = 10$ s after the video recording started is shown in Fig. 6. The data clearly show that the pendulum's oscillation amplitude in the x-direction *increases*

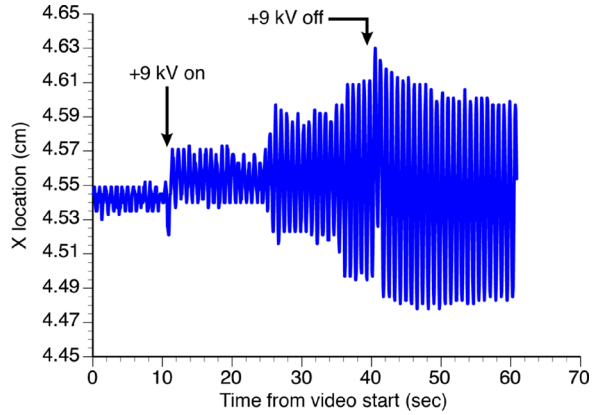

FIG. 6. X-coordinate position versus time for the electrostatic pendulum when +9 kV was applied to the pendulum with respect to ground at $t = 10$ s and gradually removed starting at $t = 39.8$ s. The current record for this experiment shows a fairly steady average current of 2 μA, and the voltage was constant within $\pm 3\%$ during the period indicated. (Due to circuit limitations, it was not possible to reduce the applied voltage to zero abruptly.).

after the high voltage is applied, and continues to do so intermittently until the voltage is gradually removed.

The most unequivocal evidence that mechanical energy is being added to the pendulum is provided by the data obtained from a 4-min run with +18 kV applied to the pendulum with respect to the platform and the chamber. To accommodate this duration, the frame rate was slowed to $3.83\ \mathrm{s}^{-1}$, which is nevertheless faster than the minimum-sampling (Nyquist) rate of $2f_0 = 2.48$ Hz required if no information with frequency components higher than $f_0 = 1.24$ Hz is to be lost. Because of the relatively high Q of the mechanical system, most of the useful information appears as sidebands on either side of the resonant frequency f_0, so little important information was lost by slowing the sample rate by a factor of four compared to the 1-min runs.

However, for purposes of illustration and data analysis, it is necessary to interpolate between actual data points to determine the cycle-by-cycle amplitude and phase of the x- and y-direction pendulum excursions. A MATLAB™ program was written to fit every sequential triplet of data points to an offset sine wave at the previously measured oscillation frequency, measured by counting cycles over the entire duration of the power-on period. For every triplet of data points, the sine wave's phase ϕ, amplitude A, and offset C were made optimization variables, and values for these three variables were found that produced a best fit to the three data points. The initial estimates for ϕ, A, and C for the following triplet of data points were set to those that were found for the previous triplet. Because these variables were generally slowly varying functions of time, this procedure for finding interpolation points worked well in general. A 5-s sample of the x-deviation from the power-on neutral point versus time, showing both the experimental data points and the 20-point-per-triplet interpolated curve, is shown in Fig. 7. The good fit in Fig. 7 is typical for most of the data. This interpolation program was used to generate the graphs of the 4-min run shown in Figs. 8 and 9. For clearer presentation, only the deviations from the power-on neutral point are shown in these figures.

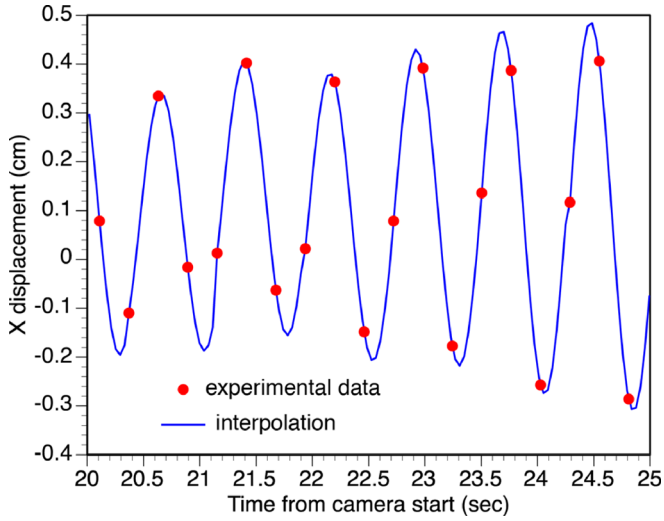

FIG. 7. 5-s selection of data from 4-min run with +18 kV on the pendulum showing experimental data points sampled at $3.83\ \mathrm{s}^{-1}$ rate and interpolated curve.

While the growth of both the x and y oscillation amplitudes is not steady, the trend is nevertheless clear. Some interaction between the x and y oscillation modes is evident and will be discussed below. However, the total energy (kinetic + potential) of the pendulum clearly grows during the 4-min experimental run, and we attribute this growth to an EHD force whose direction changes with air motion relative to the pendulum in such a way as to add energy to the pendulum.

IV. DISCUSSION

The linearized small-angle differential equations for pendulum motion in two orthogonal directions x and y corresponding to the two eigenmodes of the system are[7]

$$\frac{d^2x}{dt^2} + \frac{F_d}{m}\frac{dx}{dt} + \frac{g_{eff}}{l_x}x = 0, \tag{1}$$

$$\frac{d^2y}{dt^2} + \frac{F_d}{m}\frac{dy}{dt} + \frac{g_{eff}}{l_y}y = 0, \tag{2}$$

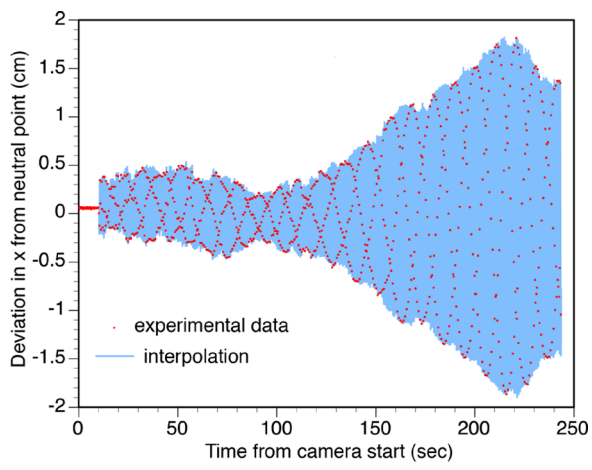

FIG. 8. Deviation from x neutral point (in cm) versus time for the electrostatic pendulum with +18 kV applied at $t = 10$ s.

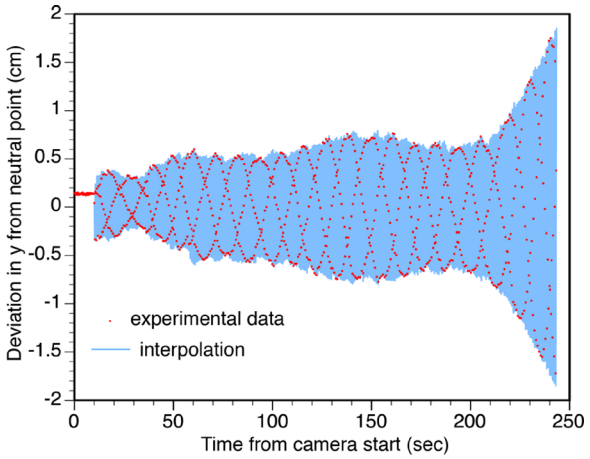

FIG. 9. Deviation from y neutral point (in cm) versus time for the electrostatic pendulum with +18 kV applied at $t = 10$ s.

where m = pendulum mass (kg), g_{eff} = effective acceleration of gravity (m s^{-2}), F_d = (linearized) frictional drag force coefficient (kg s^{-1}), and l_x, l_y are the effective lengths of the pendulum in the x and y directions, respectively, leading to two different eigenmode frequencies ω_x and ω_y. While an ideally axially symmetric pendulum would have a single effective length ($l_x = l_y = l$), it is difficult to construct a mechanical pendulum whose orthogonal oscillation modes (eigenmodes) are perfectly degenerate, as H. Kamerlingh Onnes explained in his 1879 dissertation.[8] Any slight asymmetry lifts the degeneracy of the two modes, which consequently have slightly different eigenfrequencies. The consequences of non-degeneracy do not affect the main conclusions of this analysis and will be explained below.

The effective acceleration of gravity g_{eff} is the sum of the true acceleration of gravity (9.8 m s^{-2}) and a term representing the average effect of the net downward electrostatic force on the pendulum's frequency. The mainly downward electrostatic attraction between the pendulum weight and the platform adds to the effect of gravity, and slightly raises the pendulum's resonant frequency f_0 when a high voltage of either polarity is applied. This effect was noted and taken into account in the analyses to be described.

While a pendulum with two degrees of freedom is more complex to analyze than one having only one degree of freedom, the present setup demonstrates that the effect under study is not an artifact of constraints on the pendulum's motion, but operates freely in two dimensions.

The effect of the non-degeneracy of the x and y modes has the following consequence. Assuming for the moment no losses ($F_d = 0$), let the average radian frequency of the two eigenmodes be $\omega_0 = (\omega_x + \omega_y)/2$, and half the difference be $\delta = (\omega_x - \omega_y)/2$. Then, the equations of motion for the pendulum in the x–y plane are for a particular set of initial conditions[8]

$$x(t) = A_x \sin(\omega_0 t + \delta t) \tag{3}$$

and

$$y(t) = A_y \sin(\omega_0 t - \delta t), \tag{4}$$

where A_x and A_y are the amplitudes of each eigenmode. If the two eigenfrequencies are very close together, $\delta \ll \omega_0$. Unless the pendulum is fortuitously excited in only one eigenmode (a virtually impossible eventuality), both eigenmodes will be excited in the general case. If the term δt is considered as a slowly varying phase shift, it is easily seen from Eqs. (3) and (4) that the sinusoidal x and y excitations will go in and out of phase with a period of $2\pi/\delta$, which can be on the order of seconds to minutes. The pattern traced by the pendulum in the x-y plane will be a Lissajous figure resembling the side-view projection of a tilted ring rotating on a vertical axis (see Fig. 4.12 in Ref. 7), and in the interpolated experimental data of our experiment we see just such patterns.

In general, the arbitrarily chosen orthogonal laboratory x and y coordinates will not correspond to the pendulum's natural orthogonal eigenmodes. In the extreme case when the laboratory x-y frame is at a 45° angle to the natural eigenmodes, the effect will be that energy appears to transfer from one coordinate to the other and back again. Without needlessly complicating the discussion to account for an effect that has no significant consequences for the main conclusions of the analysis, we simply state that the system's slightly different eigenfrequencies help explain why energy slowly appears to transfer between the x and y axes over a period of many hundreds of cycles, corresponding to a value of $\delta < 0.01$. Other effects such as the nonlinearity of the EHD effect can also lead to inter-mode coupling as well, but the non-degeneracy of the two eigenmodes is the most likely cause with relatively short pendulums.

While the aerodynamic drag is normally a quadratic function of stream velocity, not linear, the effect of drag for a particular amplitude of swing can be expressed in terms of an effective or equivalent linear drag coefficient F_d. Assuming for simplicity that Eqs. (1) and (2) have the same eigenfrequency ($\delta = 0$) and that the frictional loss is so small that its effect on the eigenfrequency can be neglected, each equation has a solution of the same form

$$x(t) = A_x \sin(\omega_0 t + \phi_x) e^{-\alpha/2t}, \tag{5}$$

$$y(t) = A_y \sin(\omega_0 t + \phi_y) e^{-\alpha/2t}, \tag{6}$$

where the damping coefficient $\alpha = F_d/m$ has the dimensions of s^{-1}. Even if the frictional forces are nonlinear with respect to velocity, equations such as (5) and (6) will still apply to the system, the only difference being that the damping coefficient α will be a function of amplitude. Nevertheless, for a particular experimental run, one can usually find a constant value of α that fits the experimental data.

A quantity of special interest is the total energy $U_{TOT} = U_K + U_P$, where kinetic energy is a function of velocity v

$$U_K = mv^2/2 = \frac{m}{2}\left[\left(\frac{dx}{dt}\right)^2 + \left(\frac{dy}{dt}\right)^2\right], \tag{7}$$

and potential energy

$$U_p = mg_{eff}h \cong \frac{mg_{eff}}{2l}(x^2 + y^2), \tag{8}$$

in which Eq. (8) uses the small-angle approximation to the vertical height h (m) above the neutral point in terms of

horizontal distance $r = (x^2 + y^2)^{1/2}$ from the neutral point.[7] Combining Eqs. (7) and (8) and using the derivatives of Eqs. (5) and (6) plus the expression for the pendulum's radian oscillation frequency ω_0, we find that the only information needed at any time to determine the total energy due to both motion and position away from the neutral point are the frequency, the mass, and the two amplitude coefficients in Eqs. (5) and (6)

$$U_{TOT} = \frac{m\omega_0^2}{2}\left(A_x^2 + A_y^2\right). \tag{9}$$

Accordingly, we used the $A_x(t)$ and $A_y(t)$ values found with the MATLAB interpolation program to evaluate $U_{TOT}(t)$ for a 1-min experimental run after the +18 kV source had decayed to less than 1 kV, leaving the pendulum essentially free of all electric forces and allowing its oscillations to decay due purely to mechanical losses. Figure 10 shows both the experimentally derived value of $U_{TOT}(t)$ and an exponentially decaying theoretical curve that is the best fit to the experimental data in the least-square sense. The experimental U_{TOT} data is fairly noisy due to small position errors that influence the amplitude values determined by the interpolation program, but the downward trend is clear. Using $U_0 = 208$ nJ, $t_0 = 36.1$ s (the time at which the influence of the electric field became negligible), and $\alpha = 6.82 \times 10^{-3}\,\mathrm{s}^{-1}$, we obtained the least-square best fit to the experimental data shown:

$$U_{TOT}(t) = U_0 \exp\left[-\alpha(t - t_0)\right]. \tag{10}$$

A low-loss resonator is often characterized by its quality factor Q, defined most generally as 2π times the ratio of energy stored to energy dissipated per cycle. It can be shown that for the present formulation, $Q = \omega_0/\alpha$. Thus, a determination of the damping coefficient α leads directly to a value for the mechanical oscillator's $Q = 1141$. As with most reasonably well-designed pendulums operating in air, much of the energy loss can be attributed to the drag on the ball and the suspension wire due to motion through the air.

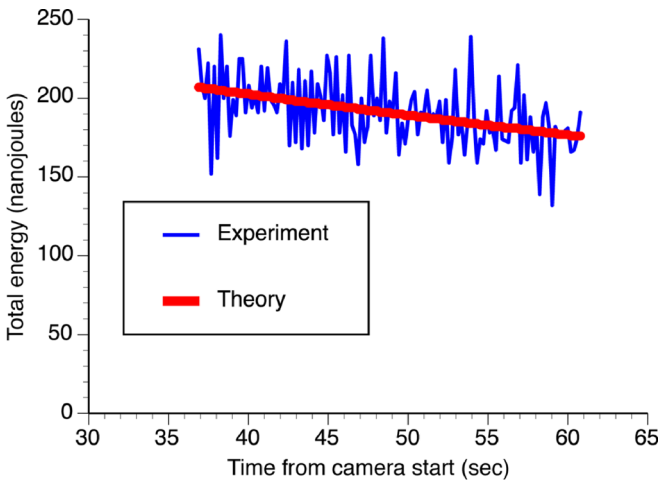

FIG. 10. Experimentally determined value of total pendulum energy U_{TOT} (thin line) and least-square fit to exponentially decaying theoretical curve (thick line) for pendulum without electric forces (mechanical losses only).

The same approach of fitting an exponential function to the experimental curve of total energy can be used to estimate the magnitude of the net transverse (horizontal) EHD force on the pendulum which is responsible for the increasing amplitude of oscillations. We performed the MATLAB interpolation operation on the experimental data of Figs. 8 and 9 for the 4-min run with +18 kV on the pendulum. The resulting total energy graph versus time is shown in Fig. 11.

While the experimental total-energy curve is both noisy and somewhat irregular, the overall trend fits reasonably well with an exponential fit of the form of Eq. (10). The coefficients used for the exponential fit in Fig. 11 were $U_0 = 479$ nJ, $t_0 = 10$ s, and the damping coefficient $\alpha = -15.255 \times 10^{-3}\,\mathrm{s}^{-1}$.

A negative damping coefficient corresponds to a force that aids, rather than opposes, the motion of the pendulum. Because an exponentially increasing curve fits the experimental data better than a linear curve, the energy added must be a function of the pendulum's velocity. If the pendulum received a constant amount of energy in each cycle regardless of the oscillation amplitude, the total energy would grow linearly rather than exponentially.

We now present our explanation for the mechanism by which EHD forces produce a net increase in pendulum energy for the duration of the experiment. As Martins and Pinheiro[9] have shown, the forces on the physical structure of an EHD experiment can be either fluid-dynamic, due to pressure differences resulting from the ion-induced motion of fluid; or electrostatic, due to attractive and/or repulsive forces between charged elements of the structure and regions of unipolar ionic charge in the fluid. Flow visualization with a source of smoke held near the corona-producing portion of the suspension wire in our experiment showed that the air flow around the system is primarily directed downward toward the platform, as the photo of Fig. 12 indicates.

First, assume the pendulum is motionless in still air and positioned at its power-on neutral point, with a positive corona-producing potential applied to it. The flow of positive-ion-bearing air around and below the pendulum will be approximately symmetrical, as shown in Fig. 13(a).

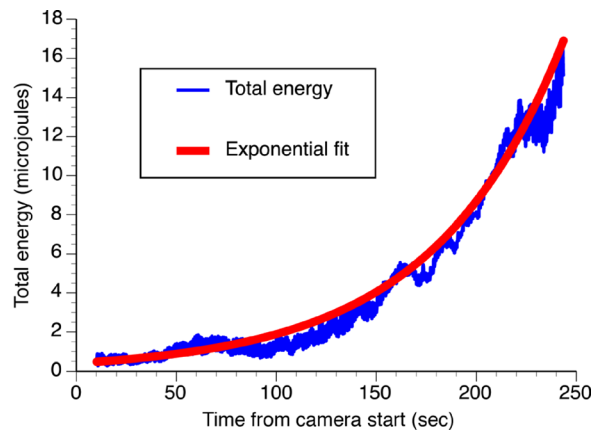

FIG. 11. Total energy U_{TOT} versus time from camera start for the 4-min run whose positions versus time were shown in Figs. 8 and 9. Note that the vertical scale is in microjoules. Coefficients of exponential fit are discussed in the text.

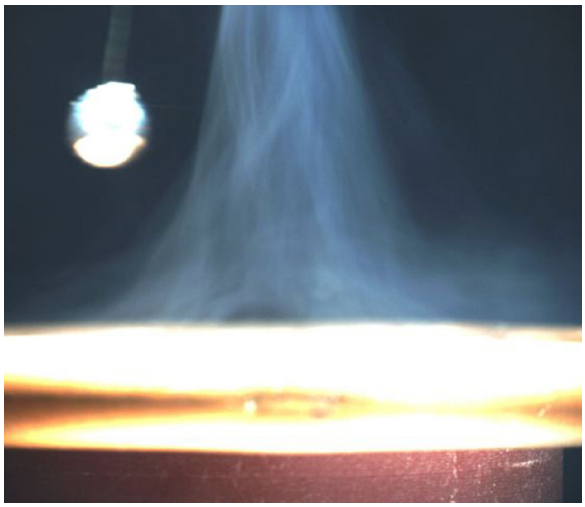

FIG. 12. Photo of smoke from the source above the frame (not shown) visualizing airflow when the pendulum is at +15 kV with respect to the platform and chamber, showing downward and outward streamlines as the flow encounters the platform.

Assuming the pendulum is positive with respect to its surroundings, the ions escaping from the corona region will also be positive and will exert a repulsive force on the pendulum, primarily the ball-bearing weight. By symmetry, however, this force will be vertical, and if the bulk of the unipolar ion cloud lies beneath the pendulum weight, the net force F_{ions} due to the unipolar ion cloud will be upward, with no horizontal component.

Next, assume we are in the frame of motion of the pendulum weight, and we examine conditions when the pendulum is vertical and moving to the left in the laboratory frame. In the pendulum frame, the pendulum experiences a flow of ambient air of velocity u_{air} directed toward the right, as shown in Fig. 13(b). This flow will add its vector velocity to the generally downward-directed flow vectors due to the ion-induced airflow of Fig. 13(a). The resultant airflow will produce a unipolar ion cloud that is skewed to the right, as Fig. 13(b) shows. As a consequence, the repulsion force vector for the moving pendulum will tilt toward the left, and will have a horizontal component *in the direction of the pendulum motion* in the laboratory frame.

The flow-visualization smoke experiments allowed us to estimate roughly the average downward airflow velocity, which is about 30 cm s^{-1} with +15 kV applied to the pendulum. The largest velocity attained by the pendulum weight in the 4-min experiment described above was about 16 cm s^{-1}. Therefore, the velocities of the ion-induced downward flow and the motion-produced flow of ambient air around the pendulum are comparable. As the pendulum velocity and amplitude increase, the diagram of Fig. 13(b) indicates that the horizontal component of the vector F_{ions} will also increase, with other things being equal. This is consistent with the conclusion we drew from the exponential shape of the increasing-amplitude curve, namely, that the force aiding the pendulum oscillations is a function of velocity.

While this qualitative analysis is imprecise, it explains the basic characteristics of the phenomenon studied. A detailed analysis of this effect, similar to what was done in e.g. Martins and Pinheiro,[9] would require 3-D dynamic modeling with continuously moving boundary conditions, and is beyond the scope of the present paper, although such an analysis could be performed in a future work.

An approximate estimate of the magnitude of the force that is exerted on the pendulum while its oscillation amplitude grows exponentially can be made by hypothesizing this expression for the horizontal component of the electrostatic force on the pendulum due to the unipolar ion cloud

$$F_{ions} = mu_{air}\beta_{ion}, \tag{11}$$

in which u_{air} is the velocity of ambient air relative to the pendulum and β_{ion} is a force coefficient analogous to the α coefficient of the linearized friction analysis above. However, the coefficient β_{ion} must be negative, and of such magnitude as not only to overcome all the friction represented by α, but to add a net amount of energy in each cycle to account for the exponentially growing oscillation amplitude. In order for this to be the case, the value of β_{ion} must be sufficiently negative to change the exponential coefficient in Eq. (10) from $\alpha = +6.82 \times 10^{-3}\,s^{-1}$ to the negative exponential coefficient taken from the data of Fig. 11, where $\alpha' = -15.255 \times 10^{-3}\,s^{-1}$. This leads to a value of $\beta_{ion} = -22.07 \times 10^{-3}\,s^{-1}$. Equation (11) gives a peak force of 3.04 μN exerted on the pendulum in this analysis when its velocity reaches the maximum value of 16 cm s^{-1}.

It is interesting to compare this value with the theoretical thrust in the vertical direction that this system could produce.

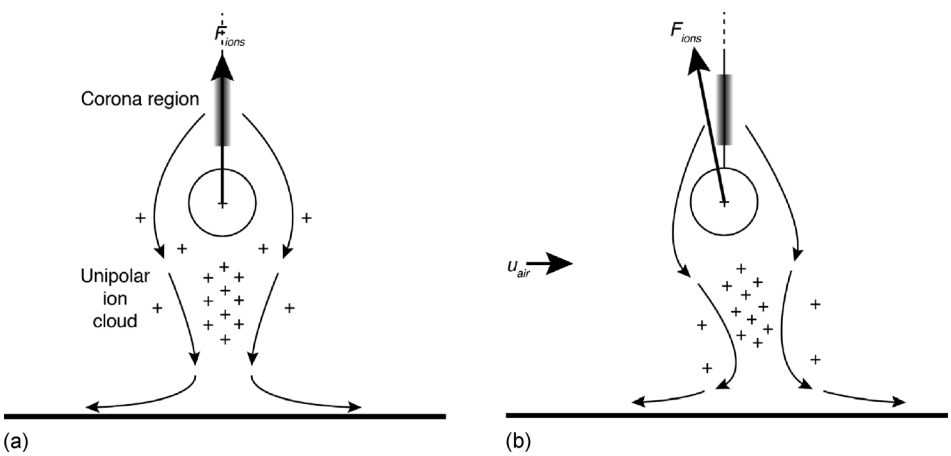

FIG. 13. (a) Airflow for the stationary pendulum, showing symmetrical distribution of the unipolar ion cloud in the absence of pendulum motion. Resultant repulsive force F_{ions} of the ion cloud on like-charged pendulum weight is directed vertically upward. (b) Airflow in the pendulum frame of motion, showing air velocity u_{air} directed toward right and resulting skewing of unipolar ion cloud toward right. Resultant repulsive force F_{ions} now has a horizontal component in the direction the pendulum is moving (toward left).

Gilmore and Barrett[10] state the result from a one-dimensional theoretical analysis, that the thrust T (N) of an EHD system in which a current I of ions with mobility μ flows between electrodes spaced a distance L apart is given by

$$T = \frac{IL}{\mu}. \tag{12}$$

If we use the maximum current measured in these experiments of $I = 19\ \mu$A, a typical room-temperature ionic mobility of $\mu = 2 \times 10^{-4}\ \mathrm{m^2\ V^{-1}\,s^{-1}}$, and the distance between the bottom of the pendulum weight and the platform as $L = 16$ mm, the vertical thrust calculated from Eq. (12) is about 1.5 mN. Equation (12) gives the value of an EHD force for a perfectly symmetrical geometry with a constant distance L between a corona wire and a parallel oppositely charged or grounded (non-ion-emitting) electrode. The geometry described in this experiment is much more complicated than the simple idealized configuration to which Eq. (12) applies, in which the force calculated is attractive instead of repulsive. The value of 1.5 mN is an estimate for the total force available in the ideal case before it is decomposed into a mainly vertical and a much smaller horizontal component, only the latter of which is responsible for the increase in the pendulum's velocity.

This approximate analysis shows that the asymmetry introduced into the unipolar ion cloud below the pendulum by pendulum motion could produce a horizontal thrust in the direction of motion that is at least 0.1% of the maximum vertical thrust estimated from Eq. (12). While this is not a quantitative confirmation of our explanation, it shows that the basic reasoning is probably correct.

V. CONCLUSIONS

We have shown how a simple electrostatic pendulum can "self-excite" and exhibit oscillations of exponentially growing amplitude by means of EHD forces under the influence of a corona discharge on the suspension wire. The effect is robust and appears whenever appreciable corona current is present. Because the pendulum is sensitive to small forces synchronized with its period, we were able to measure forces on the order of micronewtons that are responsible for an exponentially increasing oscillation amplitude over a period of minutes.

This research was undertaken as part of a program to investigate experimental models for ball-lightning motion. Wu[11] and Shmatov[12] have proposed theoretical explanations of ball lightning which indicate that ball lightning objects may emit high-energy electrons and gamma rays. If an asymmetrical cloud of unipolar ions appears in the vicinity of ball lightning, an EHD body force similar to the one demonstrated by these experiments could explain the unusual motion of ball lightning reported by many eyewitnesses: erratic, mainly horizontal movements that appear to be affected by nearby objects.[13]

ACKNOWLEDGMENTS

We gratefully acknowledge the assistance of the anonymous reviewer of an earlier version of this paper who provided the correct interpretation of the EHD force mechanism. This work was partially supported by the U.S. Department of Education's HSI STEM program (84.031c) Award No. P031C160036. We also thank Stan McClellan, Director of the Ingram School of Engineering, for support, and Pamela Stephan for photographic assistance.

[1]M. Gourdine, Trans. N. Y. Acad. Sci. **30**, 804 (1968).
[2]K.-S. Choi, T. Jukes, and R. Whalley, Philos. Trans. R. Soc. A **369**, 1443 (2011).
[3]K. Masuyama and S. R. H. Barrett, Proc. R. Soc. A **469**, 20120623 (2013).
[4]V. A. Saranin, Phys.-Usp. **55**, 700 (2012).
[5]A. Fridman and L. A. Kennedy, *Plasma Physics and Engineering*, 2nd ed. (CRC Press, Boca Raton, FL, 2011), p. 568.
[6]J. D. Cobine, *Gaseous Conductors: Theory and Engineering Applications* (Dover Publications, New York, 1958), p. 256.
[7]G. L. Baker and J. A. Blackburn, *The Pendulum: A Case Study in Physics* (Oxford University Press, Oxford, UK, 2005).
[8]E. O. Schulz-Dubois, Am. J. Phys. **38**, 173 (1970).
[9]A. A. Martins and M. J. Pinheiro, J. Electrost. **69**, 133 (2011).
[10]C. K. Gilmore and S. R. H. Barett, Proc. R. Soc. A **471**, 20140912 (2015).
[11]H.-C. Wu, Sci. Rep. **6**, 28263 (2016).
[12]M. L. Shmatov, J. Plasma Phys. **69**, 507 (2003).
[13]M. Stenhoff, *Ball Lightning: An Unsolved Problem in Atmospheric Physics* (Plenum Press, New York, NY, 1999).